



# A comparison of Car–Parrinello and Born–Oppenheimer generalized valence bond molecular dynamics

Douglas A. Gibson, Irina V. Ionova, Emily A. Carter

*Department of Chemistry and Biochemistry, University of California, 405 Hilgard Avenue, Los Angeles, CA 90095-1569, USA*

Received 20 February 1995; in final form 26 April 1995

---

## Abstract

Two methods for performing ab initio molecular dynamics using a generalized valence bond electronic wave function are compared: the Car–Parrinello and Born–Oppenheimer approaches. These techniques differ in how they generate a new electronic wave function at each time step. In the Car–Parrinello scheme, the wave function parameters are propagated as classical degrees of freedom, while in the Born–Oppenheimer scheme the equations describing the wave function are solved at each time step. It is found that trajectories obtained utilizing the Born–Oppenheimer approach are both more accurate and less costly than their Car–Parrinello counterparts for wave functions expressed in terms of atom-centered basis sets.

---

## 1. Introduction

Molecular dynamics (MD) simulations generate trajectories in phase-space by treating the nuclei classically and integrating Newton's or Hamilton's equations of motion numerically. Conventionally, the forces in the system are derived from a potential energy function which is ideally a good approximation to the true potential energy of the system. It is often the case, though, that an accurate potential function is not available, especially when it is not even clear physically what the form of that potential function should be; metal clusters are a good example of such a case. In order to perform MD simulations for such a system, we need an alternate means of calculating internuclear forces. In ab initio molecular dynamics (AIMD), that means is a first-principles quantum mechanical calculation. An AIMD trajectory does not require a potential function; instead

the energy and forces are computed directly from the quantum mechanics at each point on the trajectory. The main drawback of AIMD is that it is quite computationally intensive.

Car and Parrinello pioneered the ingenious approach of treating the parameters describing the electronic wave function as classical degrees of freedom and propagating them as such, instead of solving directly for the wave function at each step [1]. In the context of density-functional theory (DFT) based AIMD, their method significantly reduced the amount of computer time necessary per time step. By contrast, Landman and co-workers [2] and Wentzcovitch and Martins [3] took the approach of solving the Kohn–Sham equations for a new wave function each time step instead of performing fictitious dynamics on the wave function. This approach is sometimes referred to as Born–Oppenheimer dynamics, since it ensures that the system remains on the Born–Op-

penheimer potential energy surface throughout the propagation. They reported that although more computer time is used per time step to solve for the DFT wave function, doing away with the fictitious wave function dynamics allows the use of a much longer time step, and the overall efficiency is comparable to that of the Car–Parrinello method when plane-wave basis sets are employed. Chelikowsky and co-workers have applied Langevin dynamics to Born–Oppenheimer DFT-AIMD [4]. Arias, Payne, and Joannopoulos have extended Born–Oppenheimer DFT-AIMD to systems with large length scales [5]. Different implementations of DFT-AIMD have been applied to a variety of problems, utilizing both the Car–Parrinello and Born–Oppenheimer techniques [6–8].

We have developed the AIMD method for Hartree–Fock (HF) [9], generalized valence bond (GVB) [10,11], and full configuration interaction (FCI) [12] electronic wave functions, using a basis set of atom-centered Gaussian functions. Because our basis functions move with the nuclei on which they are centered, this method has the disadvantage that the integrals over basis functions which appear in the energy and force expressions must be recalculated at every time step, which is not necessary in plane-wave-based DFT-MD. In GVB-AIMD, we find that the calculation of the analytic gradient takes the vast majority of the computer time in the simulation, while calculation of the integrals accounts for the bulk of the remaining time. The full analytic gradient is necessary because forces derived from the Hellmann–Feynman theorem are often a very poor approximation with a Gaussian-based HF, GVB, or FCI wave function, while the Hellmann–Feynman forces are adequate with a plane-wave-based DFT wave function. Although these facts make DFT-AIMD significantly less expensive than GVB-AIMD, we believe that investigation of AIMD with Gaussian basis sets is still valuable due to deficiencies that remain in the DFT method, such as a lack of rigorous treatment of excited states.

In previous work, we have reduced the cost of Car–Parrinello-type HF- and GVB-AIMD by implementing the multiple time step integrator r-RESPA (reversible reference system propagator algorithm) of Tuckerman, Berne, and Martyna [13]. By taking advantage of the natural separation of electronic and

nuclear time scales, the amount of computer time needed to perform GVB-AIMD can be reduced by more than an order of magnitude [14,15]. In DFT-AIMD, solving the Kohn–Sham equations [16] every time step is the dominant cost, yet it has been found that a simulation which does just that can still be competitive with one which uses fictitious wave function dynamics [3]. We have therefore undertaken a comparison of these two methods for GVB-AIMD. In this Letter, we compare the efficiency and accuracy of the Born–Oppenheimer approach to that of the Car–Parrinello approach, when used to perform GVB-AIMD.

## 2. Methods and calculational details

### 2.1. General method

The details of our GVB-AIMD implementation have been published previously [10,15]. The dynamical variables are the SCF coefficients,  $c_{\mu i}$ , and the GVB-CI coefficients,  $\alpha_k$ , both of which define the electronic wave function, and the nuclear coordinates,  $R_I$ . The description of the system is completed by the basis set, which is a set of nuclei-centered Gaussians. The time evolution of the nuclear coordinates is governed by the equation of motion,

$$M_I \ddot{R}_I = - \frac{\partial E}{\partial R_I}, \quad (1)$$

where  $M_I$  are the atomic masses and  $E$  is the (total electronic plus nuclear) potential energy. This equation of motion may then be integrated numerically by any convenient integrator; in this work the velocity Verlet integrator [17] has been used.

When the Car–Parrinello method of propagating the electronic wave function parameters as classical degrees of freedom is used, fictitious masses and equations of motion for the wave function coefficients are also required [10]

$$m_{\text{SCF}} \ddot{c}_{\mu i} = - \frac{\partial E}{\partial c_{\mu i}} - \sum_{\nu, j} \lambda_{ij} c_{\nu j} S_{\mu\nu}, \quad (2)$$

$$m_{\text{GVB}} \ddot{\alpha}_k = - \frac{\partial E}{\partial \alpha_k}, \quad (3)$$

where  $m_{\text{SCF}}$  is the fictitious mass of the SCF coefficients,  $m_{\text{GVB}}$  is the fictitious mass of the GVB-CI coefficients,  $S$  is the atomic basis function overlap matrix, and  $\lambda_{ij}$  are the Lagrange multipliers needed to maintain the orthonormality of the orbitals. These equations of motion are also integrated numerically. We have observed empirically that in this propagation scheme the system generally remains very close to the Born–Oppenheimer potential energy surface [10]. We have used the Verlet integrator [18] for the electronic wave function coefficients and the SHAKE algorithm [19] to enforce orthonormality of the orbitals.

Accurate wave function propagation requires a shorter time step than is required for accurate nuclear propagation; electronic degrees of freedom naturally have a shorter time scale than nuclear degrees of freedom. In order to cut down on unnecessary nuclear force evaluations, the r-RESPA multiple time step integrator of Tuckerman, Berne, and Martyna was adapted to GVB-AIMD [15]. With this integration scheme, we were able to dramatically reduce the frequency with which the forces on the nuclei were computed, thus substantially reducing the simulation cost as well with little loss of accuracy.

## 2.2. Computational details

We have applied both the r-RESPA Car–Parinello [15] and the Born–Oppenheimer approaches to clusters of four and six sodium atoms in their ground electronic states with full analytical forces calculated at the GVB perfect singlet-pairing (GVB-PP) (2/4) and (3/6) levels of theory [11], respectively, where  $(n/2n)$  refers to the number of correlated electron pairs,  $n$ , and the total number of natural orbitals,  $2n$ , in the GVB wave functions used to describe those electron pairs. Thus all valence electrons were correlated. The basis set and effective core potential are identical to those in our previous studies [9,10,12,14,15,20]. The  $\text{Na}_4$  initial conditions were a slightly distorted planar rectangle with no initial kinetic energy. The actual minimum on the  $\text{Na}_4$  potential energy surface is a planar rhombus [21]. The  $\text{Na}_6$  initial geometry was randomly chosen in three dimensions, looking somewhat like a cis-bi-capped kite which had been distorted into the third dimension, and started with 19 mhartree of kinetic

energy. The minimum on the  $\text{Na}_6$  potential energy surface is a two-dimensional tricapped equilateral triangle [20]. The trajectories are approximately 350 and 960 fs in length, for  $\text{Na}_4$  and  $\text{Na}_6$ , respectively, except for one  $\text{Na}_4$  trajectory which was extended to 700 fs. It should also be pointed out that in order to get sufficiently accurate forces for AIMD, particularly in the Born–Oppenheimer approach, we find it necessary to use a significantly smaller ( $\approx 2$  orders of magnitude) criterion for wave function convergence than would normally be used for a single-point calculation. As a result, we have implemented a new wave function convergence algorithm in the GVB-AIMD code, orbital-based direct inversion in the iterative subspace (OB-DIIS), that was developed recently by two of us [22]. This improved both the accuracy of the wave function and the speed of convergence, which was key to the performance of the Born–Oppenheimer GVB-AIMD.

The nuclear time step in both approaches was varied from 50 atu (1.2 fs) to 1000 atu (24 fs); where r-RESPA was used to propagate the electronic wave function, the electronic time step was held constant at 5 atu (0.12 fs) and the fictitious masses of the SCF and GVB-CI coefficients were set to 300 au, approximately 140 times smaller than the mass of a sodium nucleus. The exact value of the fictitious mass is of little importance; it can be changed by an order of magnitude in either direction with minimal effect on the results of the simulation [10]. Furthermore, when r-RESPA was used, the wave function was reconverged periodically (every 14 fs for  $\text{Na}_4$ , and every 240 fs for  $\text{Na}_6$ ; the time is relatively long in the latter case to allow some classical propagation of the wave function to occur between reconvergences for the 1000 atu time step case) to ensure that the system remained near the Born–Oppenheimer surface.

## 3. Results

Conservation of total energy is a measure of the accuracy of an MD trajectory; since we are operating in the microcanonical ensemble, the energy will be conserved exactly if the numerical integration, energy, and forces are exact. In Fig. 1a, the total energy of the  $\text{Na}_6$  cluster is plotted for the trajectories obtained from our initial conditions with a nu-

clear time step of 50 atu (1.2 fs) with the r-RESPA Car–Parrinello and Born–Oppenheimer approaches. This plot is typical of those we have seen for both systems at all time step lengths used. We observe that the energy deviation of the Born–Oppenheimer trajectory is much smaller than that of the Car–Parrinello trajectory. Note also that the discontinuities are caused by reconverging the wave function; in the

Car–Parrinello case the kinetic energy of the wave function coefficients is forgotten upon reconvergence, and occasionally, due to the nature of the GVB wave function, the electronic configuration changes suddenly, causing a corresponding energy change. Fig. 1b adds the total energy versus time for both r-RESPA Car–Parrinello and Born–Oppenheimer trajectories with time steps of 100, 250,

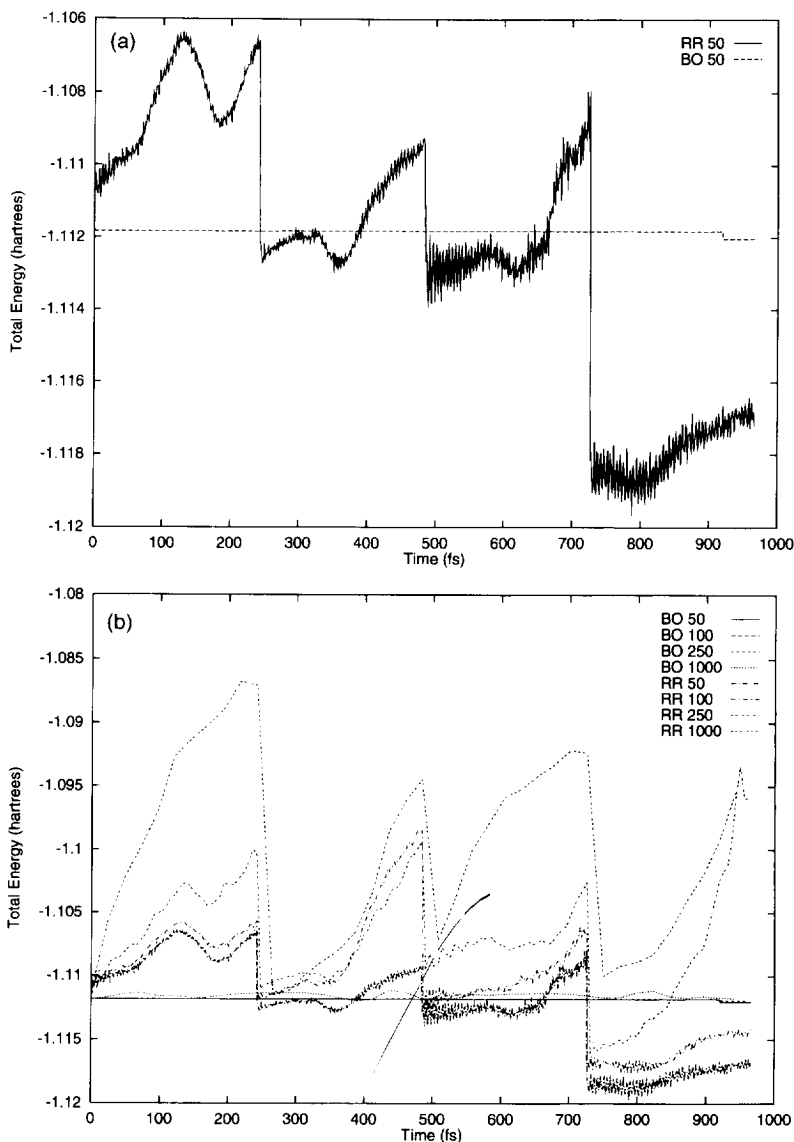


Fig. 1. (a) Total energy of two Na<sub>6</sub> trajectories as a function of time. The nuclear time step is 50 atu (1.2 fs). The solid line is Car–Parrinello with r-RESPA (RR 50 in the key), and the dashed line is Born–Oppenheimer (BO 50). (b) Total energy of eight Na<sub>6</sub> trajectories as a function of time. Nuclear time steps are 50, 100, 250, and 1000 atu. The legend denotes the type of trajectory (RR or BO) and the length of the nuclear time step (50–1000 atu).

and 1000 atu, where we see that even the longest time step Born–Oppenheimer trajectory conserves energy better than the shortest time step Car–Parrinello trajectory. Note that the 100 and 250 atu time step Born–Oppenheimer total energies are indistinguishable on this scale from the 50 atu time step total energy. Small deviations only show up for the 1000 atu time step Born–Oppenheimer trajectory.

Furthermore, the amount of computer time required to converge the wave function is sufficiently small that in this case, the Born–Oppenheimer simulation is faster. For example, the total CPU time used for 800 50 atu time steps in Fig. 1a was 61 h on an HP 735/99 workstation for the Born–Oppenheimer case and 64 h on an identical machine for the Car–Parrinello case. As the nuclear time step is lengthened, the Born–Oppenheimer approach gains a significant timing advantage (a factor of 5.4 at 1000 atu for  $\text{Na}_6$ ). We have shown previously that r-RESPA is most efficient in conjunction with our implementation of the Car–Parrinello approach when the time step ratio (nuclear time step to wave function time step) is of order 10; the speed increase is very nearly the same factor as the increase in time step ratio until it starts to level off in the region of

time step ratios of 10 to 20 [15]. This plateau in the r-RESPA Car–Parrinello performance is due to the fact that only the nuclei are being propagated less often, while the wave function must still be propagated with a relatively short time step; eventually the calculation of the forces on the nuclei ceases to be dominant. In the Born–Oppenheimer trajectories, on the other hand, there is only one time step, so this plateau effect cannot occur.

The total energies of a series of  $\text{Na}_4$  Born–Oppenheimer trajectories are plotted in Fig. 2 together with the total energy of a single time step (for both nuclei and wave function parameters) Car–Parrinello trajectory utilizing a shorter time step, 5 atu, than was used in any of the Born–Oppenheimer trajectories. Note the energy scale, the energy deviations observed are on the order of  $\mu\text{hartree}$ . These deviations would be completely invisible on the mhartree scale of Fig. 1. Discontinuities in the Car–Parrinello energy are again entirely due to changes in the fictitious electronic wave function coefficient kinetic energy upon reconvergence of the wave function. The initial large oscillation in the total energy in the 300 atu time step trajectory is due to a relatively large initial repulsion between two pairs of sodium

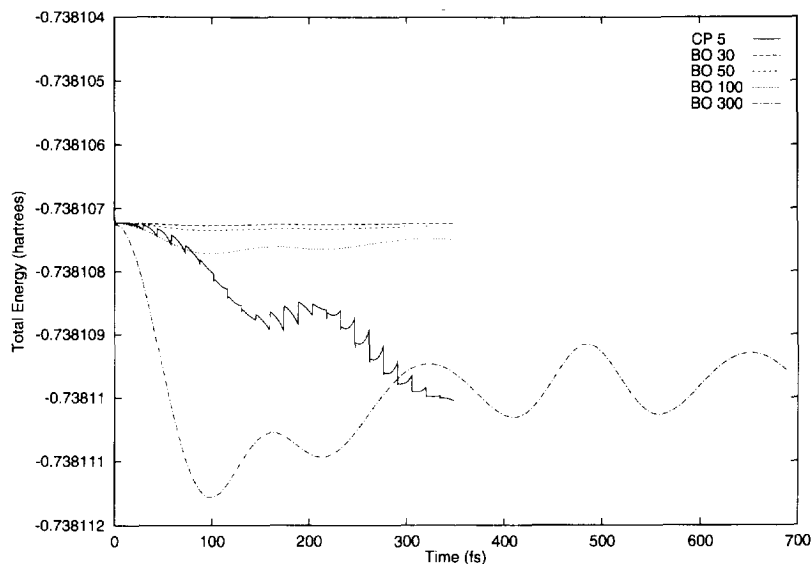


Fig. 2. Total energy of five  $\text{Na}_4$  trajectories as a function of time. The solid line is a Car–Parrinello single time step result, and the dashed lines are Born–Oppenheimer results. Again, the type of trajectory and time step length in atu is indicated in the key. Note that the Born–Oppenheimer time steps are significantly longer than the Car–Parrinello time step and note the expanded energy scale compared to Fig. 1.

atoms. Since the force tends to change rapidly for molecular systems as the system moves from the repulsive wall toward its minimum, it is not surprising that the numerical integration of the equations of motion should be more inaccurate in this region than elsewhere on the potential energy surface, and therefore the total energy should deviate most in this region. As we continue in the trajectory, the Na dimers lose contact, energy is conserved over time, and the only remaining fluctuation is due to the vibration of each pair separately.

We observe that the energy conservation of the Born–Oppenheimer trajectories tends to be better than that of the Car–Parrinello, with the sole exception of the trajectory with a time step of 300 atu, which is 60 times longer than that used in the Car–Parrinello trajectory. Even so, this 300 atu time step trajectory conserves energy approximately as well as the Car–Parrinello trajectory. We ascribe the improved energy conservation of the Born–Oppenheimer trajectories to the fact that the electronic wave function is closer to the exact adiabatic electronic state at any given time; instead of using a classical propagation scheme as in the Car–Parrinello method, the wave function is solved anew at each time step. Since the electronic wave function is more accurate, it follows that properties derived from it, particularly the forces on the nuclei, should also be more accurate in the Born–Oppenheimer approach.

#### 4. Summary and conclusions

We have implemented and compared the performance of the r-RESPA Car–Parrinello and Born–Oppenheimer approaches to GVB-AIMD. Although exploiting the natural time scale separation in the Car–Parrinello approach via r-RESPA improves performance drastically compared to a single time step simulation, we find that this does not make up for the fact that the total energy is poorly conserved relative to a Born–Oppenheimer trajectory, and less speed gain is realized in the r-RESPA Car–Parrinello method at large time step ratios due to the eventual dominance of wave function propagation. The Born–Oppenheimer approach gives much better energy conservation because, as we have found, an

accurate wave function is a prerequisite for accurate forces, and the wave function is only approximately correct during a Car–Parrinello simulation. As one might be concerned that our findings are particular to metal clusters, brief simulations of silicon clusters (which behave quite differently from sodium clusters due to the much more directional nature of their bonding) have also been performed, and those results are consistent with these conclusions as well. Where the comparison between the Car–Parrinello and Born–Oppenheimer simulations is concerned, these simulations give results which are qualitatively identical those we have obtained with sodium clusters. We therefore believe that our conclusions are largely independent of the system being simulated.

We have also observed that the Born–Oppenheimer simulations require less CPU time than r-RESPA Car–Parrinello simulations with the same nuclear time step. For the shortest nuclear time steps used in a Born–Oppenheimer simulation, 30 and 50 atu, we find that the CPU time used is only slightly less than is used in the r-RESPA Car–Parrinello simulations, but as we increase the nuclear time step (and thus the r-RESPA time step ratio, if we hold the electronic time step constant), the Born–Oppenheimer approach has an advantage. By the time we reach a nuclear time step of 1000 atu, the Born–Oppenheimer Na<sub>6</sub> simulation runs 5.4 times faster than its r-RESPA Car–Parrinello counterpart. In general, for small clusters or molecules with O(10) atoms, where wave function reconvergence is efficient, we expect the Born–Oppenheimer GVB-AIMD method to be far superior.

In order to conserve energy well with the Born–Oppenheimer approach, it is necessary to converge the wave function to greater accuracy than would normally be used in a single-point calculation. Our recent advance in wave function convergence algorithms, the OB-DIIS method, allowed for the needed efficiency and accuracy to make Born–Oppenheimer AIMD viable. The observed disparity in energy conservation between the two approaches is probably due to wave function error, since the Car–Parrinello approach gives an approximate wave function, yet the accuracy of the wave function at each step is critically important for GVB-AIMD. It may be possible to recover that accuracy in the Car–Parrinello approach by using a shorter time step, but prior work

has shown that r-RESPA time step ratios larger than about 40 do not give much improvement in speed, so it is unlikely that an improvement can be made in this area which will allow a r-RESPA Car–Parrinello-based simulation to give accuracy comparable to that of a Born–Oppenheimer simulation in the same amount of CPU time. We conclude that for GVB-AIMD, as well as other approaches that utilize non-space-fixed bases to describe the electronic wave function, Born–Oppenheimer AIMD is the method of choice, both in terms of accuracy and speed.

### Acknowledgements

This work was supported by the Office of Naval Research. EAC also acknowledges support from the National Science Foundation, the Camille and Henry Dreyfus Foundation, and the Alfred P. Sloan Foundation, through their Presidential Young Investigator, Teacher–Scholar, and Research Fellow Award programs. DAG thanks the National Science Foundation for a predoctoral fellowship.

### References

- [1] R. Car and M. Parrinello, *Phys. Rev. Letters* 55 (1985) 2471.
- [2] R.N. Barnett, U. Landman, A. Nitzan and G. Rajagopal, *J. Chem. Phys.* 94 (1991) 608.
- [3] R.M. Wentzcovitch and J.L. Martins, *Solid State Commun.* 78 (1991) 831.
- [4] J.R. Chelikowsky, N. Troullier and N. Binggeli, *Phys. Rev. B* 49 (1994) 114.
- [5] T.A. Arias, M.C. Payne and J.D. Joannopoulos, *Phys. Rev. B* 45 (1992) 1538.
- [6] R.N. Barnett and U. Landman, *Phys. Rev. B* 48 (1993) 2081.
- [7] X. Jing, N. Troullier, D. Dean, N. Binggeli, J.R. Chelikowsky, K. Wu, and Y. Saad, *Phys. Rev. B* 50 (1994) 12234.
- [8] M.E. Tuckerman, K. Laasonen, M. Sprik and M. Parrinello, *J. Phys. Condens. Matter* 6 (1994) A93.
- [9] B. Hartke and E.A. Carter, *Chem. Phys. Letters* 189 (1992) 358.
- [10] B. Hartke and E.A. Carter, *J. Chem. Phys.* 97 (1992) 6569.
- [11] F.W. Bobrowicz and W.A. Goddard III, in: *Methods of electronic structure theory*, ed. H.F. Schaefer III (Plenum Press, New York, 1977) p. 79.
- [12] Z. Liu, L.E. Carter and E.A. Carter, *J. Phys. Chem.* 99 (1995) 4355.
- [13] M.E. Tuckerman, B.J. Berne and G.J. Martyna, *J. Chem. Phys.* 97 (1992) 1990.
- [14] B. Hartke, D.A. Gibson and E.A. Carter, *Intern. J. Quantum Chem.* 45 (1993) 59.
- [15] D.A. Gibson and E.A. Carter, *J. Phys. Chem.* 97 (1993) 13429.
- [16] W. Kohn and L.J. Sham, *Phys. Rev.* 140 (1965) A1133.
- [17] W.C. Swope, H.C. Andersen, P.H. Berens and K.R. Wilson, *J. Chem. Phys.* 76 (1982) 637.
- [18] L. Verlet, *Phys. Rev.* 159 (1967) 98.
- [19] J.P. Ryckaert, G. Ciccotti and H.J.C. Berendsen, *J. Comput. Phys.* 23 (1977) 327.
- [20] I.V. Ionova and E.A. Carter, *J. Chem. Phys.* 100 (1994) 6562.
- [21] V. Bonačić-Koutecký, P. Fantucci and J. Koutecký, *Phys. Rev. B* 37 (1988) 4369.
- [22] I.V. Ionova and E.A. Carter, *J. Chem. Phys.* 102 (1995) 1251.